Science of Sintering, **52** (2020) 359-370

doi:https://doi.org/10.2298/SOS2003359N

UDK: 661.183.8; 546.74; 692.533.1, 631.433.2

Application of Ni(II)-alumina Composites for Electrocatalytic Reduction of 4-nitrophenol

Tatjana Novaković[1], Nadica Abazović[2], Tatjana Savić[2], Mirjana Čomor[2], Zorica Mojović[1*)]

[1]University of Belgrade, Institute of Chemistry, Technology and Metallurgy, Department of Catalysis and Chemical Engineering, Njegoševa 12, 11000 Belgrade, Republic of Serbia

[2]Vinča Institute of Nuclear Sciences, National Institute of the Republic of Serbia, University of Belgrade, Belgrade, Serbia

Abstract:

Nickel-alumina composites with various content of nickel were synthetized by sol-gel method. The characterization of samples was performed by diffuse reflectance spectroscopy and electrochemical impedance spectroscopy using the Mott-Schottky analysis. Glassy carbon electrode modified by synthesized composites was investigated for reduction of 4-nitrophenol. Modification of glassy carbon electrode with composite sample led to the strong apparent electrocatalysis. Principal component analysis was used to establish correlation between structural, textural and electrochemical data of investigated composites.

Keywords*: Alumina; Sol-gel processes; Electrochemical measurements, Principal component analysis.*

1. Introduction

The modification of the electrode surface by carbon based materials [1], noble metals [2], oxides [3] or polymers [4] was extensively investigated in order to achieve enhanced electrode activity. Modification with inorganic porous materials such as zeolites [5], clays minerals [6, 7] and alumina [8] gain much interest since these materials can act as catalyst support, preconcentration agent or catalyst of the reactions at the electrode surface. Such materials consist of a variety of nanoarchitectures with cavities, pores, channels, etc., from microporous to mesoporous. Great number of guest's species was introduced in pores and investigated in various processes. Furthermore, studies [9] also suggested the response of the electrode is influenced by morphology (microstructure) of the electrode material. It was also noticed that the presence of alumina on the electrode surface has enhancing effect on the electrode activity [10-13]. The effect of the alumina was attributed to the stabilization of the intermediate species through adsorption on alumina or to the enhancement of a proton transfer step by alumina.

The aim of this study was to investigate the influence of textural properties of alumina on the response of alumina-modified glassy carbon electrode. The properties of obtained alumina phases depend on the precursor, method of preparation, sample history and the calcinations conditions [14-16]. The series of alumina samples with different textural

*) **Corresponding author:** zoricam@nanosys.ihtm.bg.ac.rs

properties were synthesized by variation of calcinations temperature and Ni/Al ratio. The electrocatalytic activity of synthesized composites was studied in the reaction of electroreduction of 4-nitrophenol. Principal component analysis was used to establish correlation between structural, textural and electrochemical data of investigated composites.

2. Materials and Experimental Procedures

2.1 Synthesis

Ni(II)-doped alumina composites were prepared by sol–gel method using boehmite sol as a precursor. A stable 0.05 M boehmite sol was prepared by the hydrolysis of the aluminium isopropoxide in water at 80 ^{o}C followed by peptization of the precipitate with nitric acid at 95 ^{o}C using 0.07 mol HNO_3 per mol of Al-alcoxide, according to the procedure given by Yoldas [17]. The freshly prepared boehmite sol, pure and with variable concentration of nickel nitrate solution, were mixed together and then vigorously stirred in order to obtain a homogeneous boehmite sol. The pure and the Ni-boehmite sols were then gelled at 40 ^{o}C, during 24 hours, than at 100 ^{o}C in same time interval. The gels were heated from room temperature to the final temperature of 500, 900 and 1100 ^{o}C with the heating rate of 2 ^{o}C min^{-1} and were kept at goal temperature for 5 h. The samples obtained in this manner are designated as A-500, A-900 and A-1100 for pure alumina, where A stands for alumina and the number stand for final temperature. The samples containing Ni were designated as, for example, A10-500 and so on, where A stands for alumina, the first number describes the mass% of Ni in alumina sol, and the second number stands for final heating temperature.

2.2 Sample characterization

Diffuse reflection spectra were recorded using Shimadzu UV-2600 (Shimadzu Corporation, Japan) spectrophotometer equipped with an integrated sphere (ISR-2600 Plus) in a 220-1300 nm range.

UV/Vis absorption spectra of 4-nitrophenol (4-NP) aliquots were obtained using an Evolution 600 spectrophotometer (Thermo Scientific).

The results obtained by characterization of samples by nitrogen adsorption-desorption isotherms and X-ray powder diffraction measurements are presented elsewhere [18, 19].

2.3 Electrochemical experiments

Electrochemical experiments were performed in three-electrode glass cell using Autolab electrochemical workstation (Autolab PGSTAT302N, Metrohm-Autolab BV, Netherlands). The reference electrode was Ag/AgCl in 3 M KCl, while a platinum rod served as a counter electrode. Glassy carbon electrode (GCE) with area of 0.071 cm^2 modified with synthesized alumina powder was used as working electrode. Alumina powder samples were homogeneously dispersed in original 5 wt.% Nafion solution using an ultrasonic bath. Droplets (10 μl) of these suspensions (containing 1 mg of alumina powder) were placed on the surface of a glassy carbon electrode. After solvent evaporation, the alumina was uniformly distributed on the glassy carbon support in the form of a layer. Impedance measurements were carried out at constant potential using a 5 mV rms sinusoidal modulation in the 10 kHz-10 MHz frequency range in 0.1 M Na_2SO_4. Mott–Schottky measurements were performed at the frequency of 1 Hz, with the voltage applied at successive steps of 50 mV from 1 V to -1 V in 0.1 M Na_2SO_4. Cyclic voltammetry was performed at scan rate of 50 mVs^{-1} in 0.5 M H_2SO_4 with a 1 mM 4-nitrophenol.

2.4 Catalytic and photodegradation procedure

Representative degradation experiment was performed according to procedure given by Naik et al. [20]. Briefly 40 mg of alumina sample suspended in 12 ml of water and an aqueous solution of $NaBH_4$ (5 ml, 0.2 M) were rapidly introduced into an aqueous solution of 4-nitrophenol (22.5 ml, 0.1 mM) and then the whole mixture was allowed to react for 2 min at room temperature under atmospheric pressure. The aliquots (1 cm^3) were taken from the suspensions in regular time intervals during 30 minutes and centrifuged prior to UV/Vis absorption spectra measurements. The concentration of 4-nitrophenol was quantified by measuring the absorption intensity at λ_{max} = 390 nm.

Photocatalytic degradation procedure was carried out at atmospheric pressure and room temperature. 20 mg of synthesized material (A10-1100) and 19 mg $NaBH_4$ were added to 20 cm^3 of 4-nitrophenol aqueous solution (concentration 10 ppm). Before illumination, the mixture was stirred in the dark for one hour in order to achieve the adsorption-desorption equilibrium. Reaction suspension was constantly bubbled with O_2 and magnetically stirred during irradiation. Suspensions were placed into a vessel which was exposed to white light from an Osram Vitalux lamp (300 W, Sun light simulation, white light: UVB radiated power from 280 to 315 nm 3.0 W; UVA radiated power 315-400 nm 13.6 W; the rest is visible light and IR). The aliquots (1 cm^3) were taken from the suspensions in regular time intervals during 1h of illumination and centrifuged prior to UV/Vis absorption spectra measurements.

2.5 Principal component analysis

Principal component analysis (PCA) was used to analyze data obtained for investigated composites. The input data were constituted of data obtained from various characterization techniques. A PCA model was constructed using all samples. The score plot of PC1 versus PC2 was examined for clustering results. Correlation matrix of investigated variables was extracted.

3. Results and Discussion

3.1 Optical characterization

In "normal" spinel structures tetrahedral sites are occupied by bivalent (Ni^{2+}) ions, while octahedral sites are occupied by trivalent (Al^{3+}) cations. However, when both cations adopt both coordinations, invers spinel structures are formed [21]. Diffuse reflectance UV-Vis/NIR spectra of synthesized materials are transformed to absorbance spectra using Kubelka Munk functionality (incorporated in operating Shimadzu software) and presented in Fig. 1.

Peaks/shoulders obtained in the spectra of composite samples can be assigned to various coordination/oxidation states of nickel species on the surface of spinel structure. Strong absorption in UV region between 220 and 370 nm present in spectra of all composite samples, with exception of sample A10-1100, originate from $O^{2-} \rightarrow Ni^{2+}$ ligand to metal charge transfer [21, 22]. Peaks at 377 and 720 nm, correspond to d-d transitions of octahedrally coordinated Ni^{2+} species in NiO lattice [21, 22]. These peaks are prominent in spectra of samples with higher content of Ni, calcined at 900 and 1100 ^oC, but not in spectra of A10 samples, regardless of calcination temperature. This leads to assumption that in samples with 10 wt% of Ni, NiO is not formed as separated phase, even after calcination at high temperatures.

Another significant difference among A10 samples and samples with higher load of nickel, is wide band in NIR region located between 850 and 1250 nm attributed to the $\nu_1(^3A_{2g} \rightarrow {}^3T_{2g})$ transition of Ni^{2+} in octahedral symmetry in nickel aluminate lattice [21, 23].

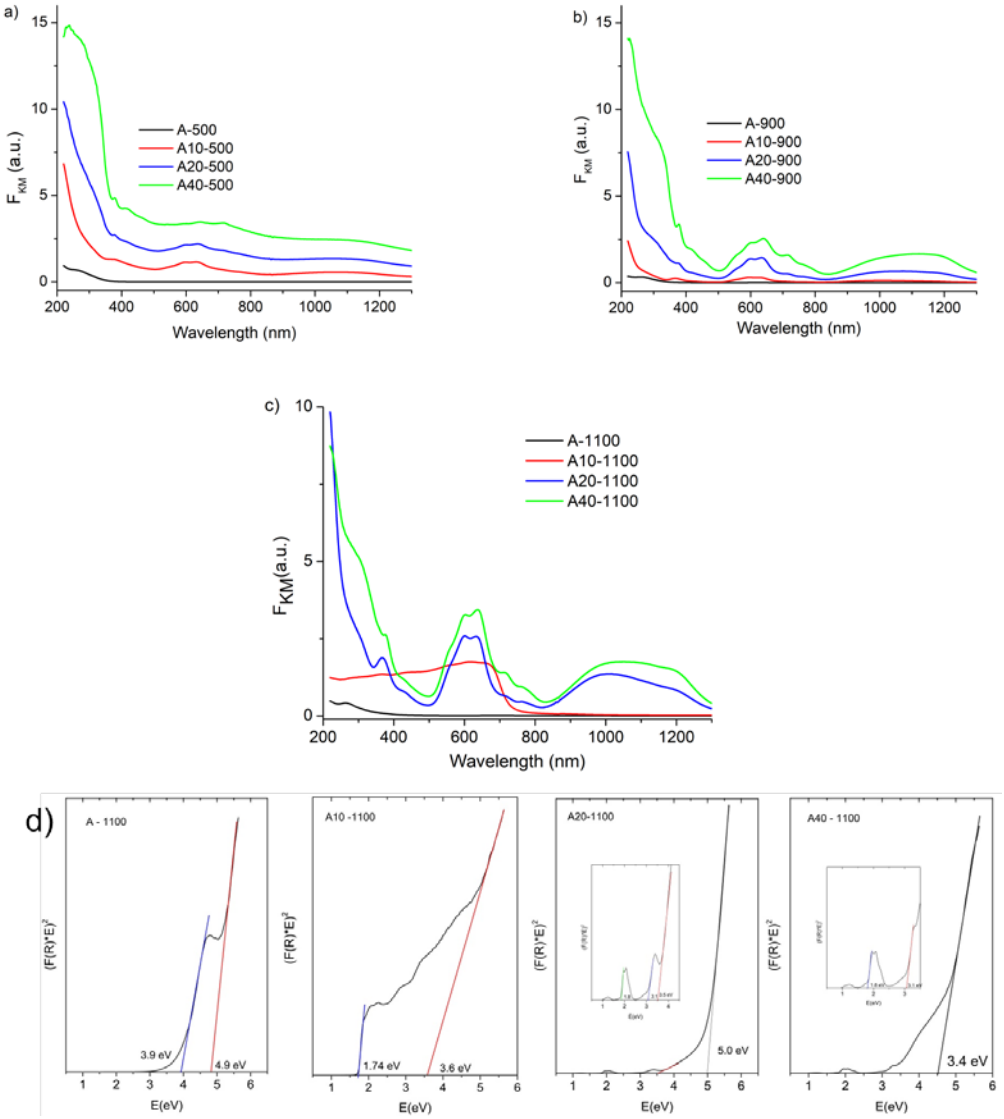

Fig. 1. UV-Vis/NIR absorption spectra of synthesized materials annealed at a) 500, b) 900 and c) 1100 ^{o}C; d) Tauc's plots of samples annealed at 1100 ^{o}C. For the sake of clarity, enlarged parts of plots in energy range from 1 to 4 eV are presented as insets.

Absorption maxima placed at 600 and 640 nm are common for all composite samples and originate from tetrahedrally coordinated Ni^{2+} species in the nickel aluminate lattice [21-23]. In order to estimate band-gap energy of alumina and composites and identify energies of electron transitions, DRS spectra were transformed to Tauc's plots (Fig. 1d). Estimated band gap energy of alumina was about 4.9 eV. However, Tauc plots are characterized by the presence of additional transition at 3.9 eV, which probably originate from defect states placed in band gap of alumina matrix. This result is in accordance with XRD data [19], which confirmed defect spinel structure of γ-alumina, characterized with the presence of cation vacancies. Extrapolation of linear part of the Tauc's plot for A10-1100 sample gave value of 1.74 eV, which is close to value reported previously for $NiAl_2O_4$ [24], but also at 3.6 eV, which corresponds to band-gap energy of NiO [25] Tauc's plot of A20-1100 sample revealed presence of alumina (5.0eV), $NiAl_2O_4$ (1.8eV) and NiO (3.6eV), with additional transition placed at 3.1 eV, which can be attributed to oxygen vacancy with one electron [26]. Tauc's

plot of sample with the highest Ni loading (A40-1100) also revealed presence of $NiAl_2O_4$ and NiO phases, but no alumina related transition is detected. Namely, in sample with a such high Ni loadings NiO crystallites can be formed initially at the surface of alumina, in which case the formation of Ni-aluminate will be retarded [27], but also, as DRS is surface related technique, presence of alumina could be somewhat hindered.

3.2 Mott-Schottky

The properties of electrode/electrolyte interface for GCE electrode modified with alumina samples was investigated by electrochemical impedance spectroscopy using the Mott-Schottky analysis. Mott-Schottky relationship is given as [28]:

$$\frac{1}{C^2} = \frac{2}{\varepsilon\varepsilon_0 eN}\left(E - E_{fb} - \frac{kT}{e}\right) \quad (1)$$

where C is the interfacial capacitance, ε is the relative electric permittivity, ε_0 is the electric permittivity of vacuum, e is the elementary charge, N is the charge carrier density, E is the applied potential, E_{fb} is the flat band potential, k is the Boltzmann constant and T is the absolute temperature.

Mott-Schottky plot gave straight line for dC/dE plot with intercept with potential axis at E_{fb}. According to Mott-Schottky plots (Fig. 2) all investigated samples showed n-type behavior.

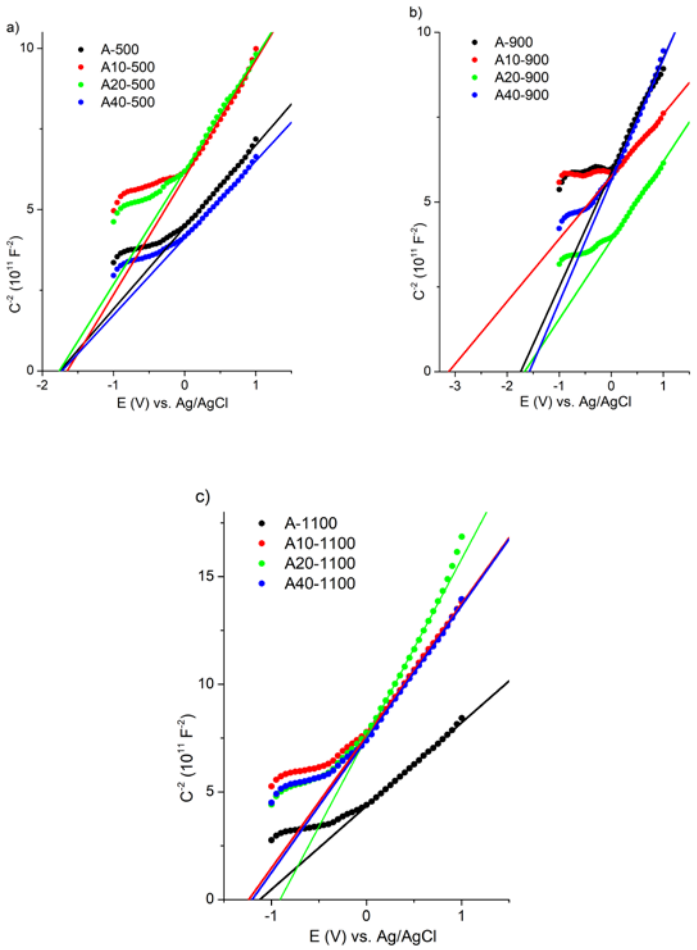

Fig. 2. Mott-Schottky plot of the samples calcined at a) 500 ^{o}C, b) 900 ^{o}C and c) 1100 ^{o}C measured in 0.1 M Na_2SO_4.

The obtained values of flat band potential are given in respect to SHE and are listed in Table I.

Tab. I Flat band potentials of investigated alumina samples determined from Mott-Schottky plots.

Sample	E_{fb} (V)
A-500	-1.75
A10-500	-1.65
A20-500	-1.76
A40-500	-1.73
A-900	-1.74
A10-900	-3.12
A20-900	-1.67
A40-900	-1.57
A-1100	-1.12
A10-1100	-1.23
A20-1100	-0.87
A40-1100	-1.20

The values of flat band potential for alumina samples calcined at 500 and 900 ^{o}C were similar to each other and around -1.7 V. The exception was A10-900 sample which exhibited extremely low flat band potential. The accumulation of the electrons on the electrode/electrolyte surface with slow charge-transfer kinetics leads to low values of flat band potentials [29]. Significant anodic shift was noticed only for samples calcined at 1100 ^{o}C indicating faster charge-transfer kinetics. Due to the phase transformation into the alpha alumina phase, the samples thermally treated at 1100 ^{o}C have significantly different surface properties and the weakest developed textural characteristics [18] compared to the samples from the other two temperature series. It might be assumed that interfacial properties originated from GCE were modified to the different degree by alumina samples.

3.3 Cyclic voltammetry

The electrochemical behavior of alumina samples toward 4-NP was tested in 0.1M H_2SO_4 (Fig. 3a-c). In order to evaluate electroactivity originating only from alumina, voltammograms of GCE and GCE covered with Nafion (GCE+Naf) were also recorded (Fig. 3d).

The cathodic peak originated from reduction of $–NO_2$ group in 4-NP was recorded on GCE at -0.68 V. The presence of Nafion on the electrode surface shifts onset of reduction potential of 4-NP toward more positive potential, although reduction current was lower. Besides, the pair of redox peaks at 0.65 V appeared originating from reversible oxidation of intermediates of $–NO_2$ reduction. According to previous research [7, 30], the peak at negative potential can be ascribed to equation (2), and reversible pair of peaks to the equation (3):

$$OH - \Phi - NO_2 + 4e^- + 4H^+ \rightarrow OH - \Phi - NHOH + H_2O \quad (2)$$

$$OH - \Phi - NHOH \leftrightharpoons OH - \Phi - NO + 2e^- + 2H^+ \quad (3)$$

Additional modification of the electrode surface by alumina samples caused further positive shift of the reduction potential of about 130-200 mV in comparison to GCE or 40-110 mV in comparison to GCE+Naf. Similar effect was noted for the pair of redox peaks at higher potential ascribed to reaction 3. Apparent electrocatalytic effect was noted for all samples, although in somewhat different degree. The only significant difference was noticed

in the height of current response along series of samples. This difference was least expressed for samples calcined at 1100 °C. Compton and co-workers [13] said that noticed effect cannot be ascribed to the electrocatalytic but to the overall catalytic effect. Similarly the catalytic effect on the adsorbed electroactive species was ascribed to the facilitating the two-electron process of catechol reduction by the presence of proton accepting oxide groups on the surface of the alumina [12]. Electrochemical response of GCE modified with different alumina samples toward 4-NP reduction was rather similar to each other. Bearing in mind that alumina samples investigated in this paper have rather different textural properties [18] and crystallographic structure [19] it can be concluded that apparent electrocatalytic effect probably originated from surface properties of alumina samples that were similar in all investigated samples. The highest currents for reversible redox peak were observed for alumina samples A10-1100.

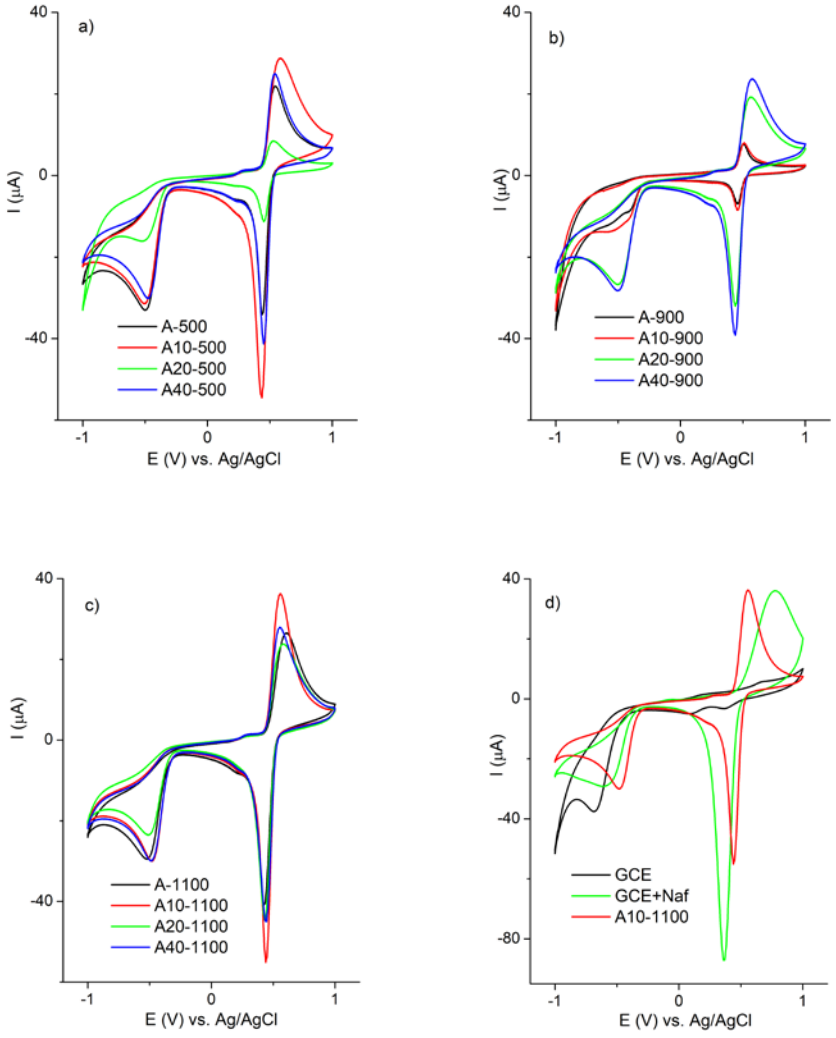

Fig. 3. Cyclic voltammograms of 1 mM 4-NP in 0.1 M H_2SO_4 recorded at scan rate 50 mVs^{-1} on GCE modified with alumina samples calcined at a) 500 b) 900 c) 1100 °C; d) Cyclic voltammograms of 1 mM 4-NP in 0.5 M H_2SO_4 recorded at scan rate 50 mVs^{-1} on GCE, GCE+Naf and GCE modified with A10-1100.

Electrocatalyst lowers overpotential for the direct transfer of electrons through the surface catalytic reaction. It is considered that the process of surface catalytic reactions in photocatalysis is very similar to electrocatalysis [31].

Parallel experiments investigating catalytic and photocatalytic properties of composites were also performed. However, investigated composites test have not showed any catalytic or photocatalytic activity. Comparing the results of the experiments it is evident that Ni-alumina composites expressed only electrocatalytic activity. The electrochemical reaction occurred on the electrode surface involving reactants that were affected by the presence of alumina. The adsorption is probably the main driving force behind the apparent electrocatalysis. Literature data [32] report that the adsorption of nitrophenol on the alumina surface does not occur through electrostatic interactions via $-OH_2^+$ groups. The adsorption proceeds through the donor/acceptor complexes, where the nitrophenol acts as the acceptor and alumina oxygen as the strong donor. The ability of the 4-nitrophenol to act as electron acceptors is the consequence of the low electron density caused by the strong electron withdrawing ability of NO_2 -group. The chemical nature of the aluminum oxide surface is one of the most important characteristics for its catalytic and adsorption properties. The properties of the surface depend on many parameters, but the crucial parameters are: nature of the material, particle morphology, and oxidation and coordination state of surface species. Coordination states are relevant for the distribution of charge (acid-base character) of surface-active centers. Thermal decomposition of crystalline hydrated forms of aluminum oxide yielded gamma phase at 500 ^oC, delta phase at 900 ^oC and stable α-Al_2O_3 at 1100 ^oC [19]. The amount of the surface hydroxyl groups is reduced with the increase of the calcination temperature. During the dehydroxylation process the leaving molecule of water, formed by the association of two adjacent OH-groups, releases two active centers: the oxygen ion, like the Lewis base center (donor e-) and aluminum ion, as the Lewis acid center (e- acceptor) [33, 34]. Introduction of nickel caused additional rearrangement of the surface due to nickel incorporation in alumina structure. The highest apparent electrocatalytic activity observed for A10-1100 sample is probably the consequence of the number of adsorption sites available for 4-nitrophenol adsorption and their arrangement on the alumina surface. Critical condition was also formation of the triple boundary formed by the electrode, the solution, and the alumina particles [12]. The noticed differences in the electrochemical behavior of Ni-alumina composites are the consequence of the adsorptive and morphological properties of the composites.

3.4 Principal component analysis

In order to have better insight which parameter has mostly contributed to the expressed electrocatalytic effect the principal component analysis was performed. Principal component analysis, as a well-known technique of multivariate data analysis, was used to analyze properties of investigated Ni-alumina composites. PCA was performed with data that take into account only properties of alumina. The influence of nickel phases on the electrocatalytic activity was previously investigated [19] in the reaction of electrooxidation of methanol. The recorded electrocatalytic activity originated only from formed NiO and was directly proportional to its amount. According to the obtained currents of methanol electrooxidation, the contribution of nickel phases to the electrocatalytic activity of composites was very low. Data matrix of data used for PCA was composed of textural and structural properties data taken from out previous publication [18, 19] and from data obtained in the present work. The obtained score plot and loading plot are presented in Fig. 4.

The first three components contained 74.1 % of all the information. The score plot presented in Fig. 4a shows that clustering of samples is predominantly governed by temperature of calcination. The only exception was sample A-1100. The loading plot (Fig. 4b) shows how recorded characteristics correlate with each other. The angle of 180^o implies

strong but negative correlation, while small angles imply strong, positive correlation. The angle of almost 90^o implies low correlation coefficient between observed vectors. Ia and Ic are positively correlated, as expected. It can be seen that the most influence on reduction current of 4-nitrophenol had the value of total pore volume ($V_{0.98}$). However, this correlation is negative, with increase of total pore volume the peak current of 4-NP decrease. On the other hand, all other investigated variables showed much lower effect on the cathodic peak current.

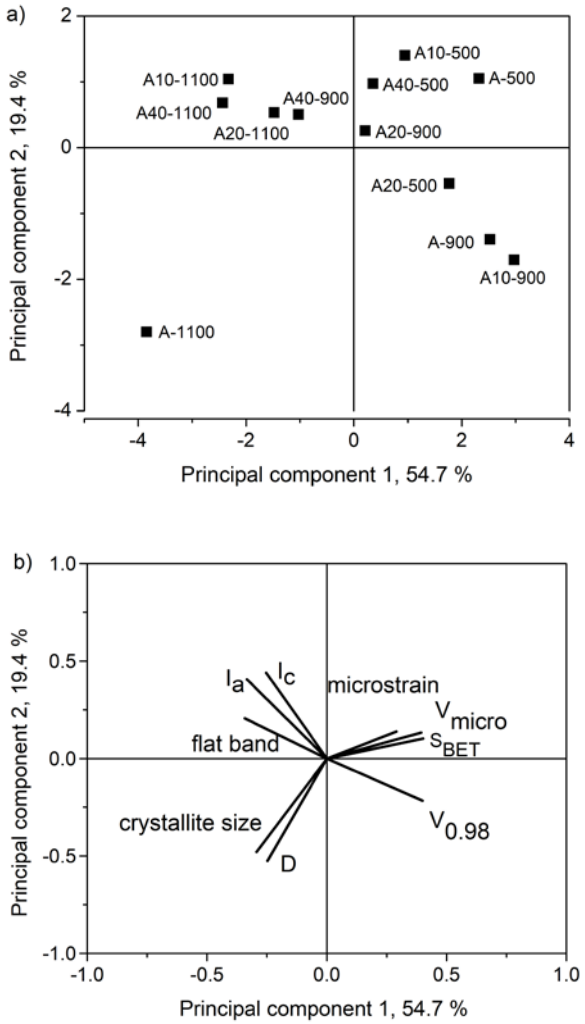

Fig. 4. a) PC1 vs. PC2 score plot; b) PC1 vs. PC2 loading plot.
I_c – cathodic peak current of 4-NP reduction; I_a – anodic peak current of oxidation of intermediate formed by 4-NP reduction; Flat band – flat band potential; Microstrain – the parameter related to the imperfection of crystal structure; V_{micro} – micropore volume;
S_{BET} - specific surface area; $V_{0.98}$ – total pore volume estimated from the amount of nitrogen adsorbed at the relative pressure of 0.98; D – the maximum pore diameter; Crystallite size – the size of alumina crystallite in nm.

According to the result of PCA, the triple boundary, inevitably formed by the electrode, the solution, and the alumina particles, was mostly affected by total pore volume.

4. Conclusion

Nickel-alumina composites were synthetized by sol-gel method and calcined at 500, 900 and 1100 ^{o}C. The characterization of samples has confirmed that the phase composition of Ni- alumina samples were dependent on the amount of Ni added and the annealing temperature. Samples with higher nickel content contained nickel as Ni-aluminate and NiO, later being formed as impurity and placed at the surface of the samples. Electrocatalytic, catalytic and photocatalytic activity of nickel-doped alumina was tested in degradation reaction of 4-nitrophenol. No catalytic or photocatalytic degradation of 4-nitrophenol was observed under employed experimental conditions. Modification of glassy carbon electrode with composites led to the strong apparent electrocatalytic reduction of 4-nitrophenol. The noticed differences in the electrochemical behavior of Ni-alumina composites were the consequence of the adsorptive and morphological properties of the composites. Principal component analysis revealed that the total pore volume had the most influence on the electrocatalytic properties of investigated composites.

Acknowledgments

This work was supported by the Ministry of Education, Science and Technological Development of the Republic of Serbia.

5. References

1. Z. Wang, P. M. Lee, E. Liu, “Graphene thin film electrodes synthesized by thermally treating co-sputtered nickel–carbon mixed layers for detection of trace lead, cadmium and copper ions in acetate buffer solutions”, *Thin Solid Films*, 544 (2013) 341-347.
2. L. Laffont, T. Hezard, T, P. Gros, L-E. Heimbürger, J. E. Sonke, P. Behra, D. Evrard “Mercury(II) trace detection by a gold nanoparticle-modified glassy carbon electrode using square-wave anodic stripping voltammetry including a chloride desorption step”, *Talanta*, 141 (2015) 26-32.
3. V. Anbumannan, M. Dinesh, R. T. Rajendra Kumar, K. Suresh “Hierarchical α-MnO_2 wrapped MWCNTs sensor for low level detection of p-nitrophenol in water”, *Ceram Int*., 45 (2019) 23097-23103.
4. L. Chen, Z. Su, X. He Y. Liu, C. Qin, Y. Zhou, Z. Li, L. Wang, Q. Xie, S. Yao,“Square wave anodic stripping voltammetric determination of Cd and Pb ions at a Bi/Nafion/thiolated polyaniline/glassy carbon electrode”, *Electrochem Commun*., 15 (2012) 34-37.
5. A. Walcarius,“Zeolite-modified electrodes: Analytical applications and prospects”, *Electroanalysis*, 8 (1996) 971-986.
6. A. Fitch,“Clay-modified electrodes: A review”,*Clay Clay Miner*., 38 (1990) 391-400.
7. N. Jović-Jovičić, Z. Mojović M. Darder, P. Aranda, E. Ruiz-Hitzky, P. Banković, D. Jovanović, A. Milutinović-Nikolića, Smectite-chitosan-based electrodes in electrochemical detection of phenol and its derivatives, *Appl Clay Sci*., 124-125 (2016) 62-68.
8. X. H. Zhao, M. Fuji, T. Shirai, H. Watanabe, M. Takahashi, Electrocatalytic evolution of oxygen on NiCu particles modifying conductive alumina/nano-carbon network composite electrode, *Sci. China Tech. Sci.*, 55 (2012) 3388-3394.
9. J. J. Huang, J. Luo, “Composites of sodium manganese oxides with enhanced electrochemical performance for sodium-ion batteries: Tailoring properties via controlling microstructure”, *Sci. China Tech. Sci.*, 59 (2016) 1042-1047.

10. J. Zak, T. Kuwana, "Electrooxidative catalysis using dispersed alumina on glassy carbon surfaces" *J. Am. Chem. Soc.*, 104 (1982) 5514-5551.
11. J. Zak, T. Kuwana, "Chemically modified electrodes and electrocatalysis" *J. Electroanal. Chem.*, 150 (1983) 645-664.
12. Q. Lin, Q. Li, C. Batchelor-McAuley, R. G. Compton, "Two-electron, two-proton oxidation of catechol: Kinetics and apparent catalysis", *J. Phys. Chem. C*, 119 (2015) 1489-1495.
13. J. Poon, Q. Lin, C. Batchelor-McAuley, C. Salter, C. Johnston, R.G. Compton, "Altered electrochemistry at graphene- or alumina-modified electrodes: Catalysis vs electrocatalysis in multistep electrode processes", *J. Phys. Chem. C*, 119 (2015) 13777-13784.
14. T. Sekino, T. Nakajima, S. Ueda, K. Niihara, "Reduction and sintering of a nickel–dispersed-alumina composite and its properties", *J. Am. Ceram. Soc.*, 80 (1997) 1139-1148.
15. Y. Chen, W. Huo, X. Zhang, Y. Lu, S. Yan, J. Liu, K. Gan, J. Yang, "Ultrahigh-strength alumina ceramic foams via gelation of foamed boehmite sol", *J. Am. Ceram. Soc.*,102, (2019) 5503-5512.
16. Z. Ecsedi, I. Lazău, C. Păcurariu,"Synthesis of mesoporous alumina using polyvinyl alcohol template as porosity control additive", *Process. Appl. Ceram.*, 1 (2007) 5-9.
17. B. E. Yoldas, "Alumina sol preparation from alkoxides" *Am. Ceram. Soc. Bull.*, 54 (1975) 289-290.
18. A. Ivanović-Šašić, T. Novaković, Z. Mojović, Ž. Čupić, D. Jovanović,"Cyclic voltammetric study of the influence of porosity on electrochemical response of Nafion/alumina modified glassy carbon electrode", *Sci. Sinter.*, 50 (2018) 313-321.
19. Z. Mojović, T. Novaković, M. Mojović, T. Barudžija. M. Mitrić, "Electrochemical and structural properties of Ni(II)-alumina composites as an annealing temperature function", *Sci. Sinter.*, 51 (2019) 339-351.
20. B. Naik, V. S. Prasad, N. N Ghosh NN,"Preparation of Ag nanoparticle loaded mesoporousγ-alumina catalyst and its catalytic activity for reduction of 4-nitrophenol", *Powder Technol.*, 32 **(**2012) 1-6.
21. Z. Boukha, C. Jiménez-González, B. de Rivas, J. R. González-Velasco, J. I. Gutiérrez-Ortiz, R. López-Fonseca,"Synthesis, characterisation and performance evaluation of spinel-derived Ni/Al_2O_3 catalysts for various methane reforming reactions", *Appl. Catal. B-Environ.*, 158-159 (2014) 190-201.
22. P. Kim, Y. Kim, H. Kim, I. K, Song, J. Yi,"Synthesis and characterization of mesoporous alumina with nickel incorporated for use in the partial oxidation of methane into synthesis gas", *Appl. Catal. A-General.*, 272 (2004) 157-166.
23. M. Gil-Calvo, C. Jiménez-González, B. de Rivas B, J. I. Gutiérrez-Ortiz, R. López-Fonseca,"Effect of Ni/Al molar ratio on the performance of substoichiometric $NiAl_2O_4$ spinel-based catalysts for partial oxidation of methane", *Appl. Catal. B-Environ*., 209 (2017) 128-138.
24. I. Sebai, N. Salhi, G. Rekhila, M. Trari,"Visible light induced H_2 evolution on the spinel $NiAl_2O_4$ prepared by nitrate route", *Int. J. Hydrogen. Energ.*, 42 (2017) 26652-26658.
25. B. Sasi, K. G. Gopchandran, P. K. Manoj, P. Koshy, P. P. Rao, V. K. Vaidyan,"Preparation of transparent and semiconducting NiO films", *Vacuum*, 68 **(**2003) 149-154.
26. Z. Heiba, M. B. Mohamed, A. M. Wahba, N.G. Imam,"Structural, Optical, and Electronic Characterization of Fe-Doped Alumina Nanoparticles", *J. Electron. Mater.*, 47 (2018) 711-720.

27. B. Scheffer, J. J. Heijeinga, J. A. Moulijn,“An electron spectroscopy and X-ray diffraction study of NiO/Al_2O_3 and $NiO-WO_3/Al_2O_3$ catalysts”, *J. Phys. Chem.*, 91 (1987) 4752-4759.
28. A. J. Bard, L. R. Faulkner, *Electrochemical methods: Fundamentals and applications.* 2nd ed. New York: Wiley, 2001.
29. J. D. Beach, R. T. Collins, J. A. Turner,“Band-edge potentials of n-type and p-type GaN”, *J. Electrochem. Soc.*, 150 (2003) A899-A904.
30. D. De Souza, S. A. S. Machado,“Study of the electrochemical behavior and sensitive detection of pesticides using microelectrodes allied to square-wave voltammetry”, *Electroanalysis*, 18 **(**2006) 862–872.
31. R. Li, C. Li,“Chapter one-photocatalytic water splitting on semiconductor-based photocatalysts”, pp. 1-57. in(ed) *Advances in catalysis* eds. by C. Song Academic Press, 2017,
32. M. Aazza, H. Ahlafi, H. Moussout,H. Maghat,“Ortho-nitro-phenol adsorption onto alumina and surfactant modified alumina: kinetic, isotherm and mechanism”, *J. Environ. Chem. Eng.*, 5 (2017) 3418-3428.
33. A. Zecchina, C. Lamberti, S. Bordiga,“Surface acidity and basicity: General concepts”, *Catal. Today.*, 41 (1998) 169-177.
34. E. Giamello,“Reactive intermediates formed upon electron transfer from the surface of oxide catalysts to adsorbed molecules” *Catal. Today.*, 41 (1998) 239-249.

Сажетак: *Никл-алумина композити са различитим садржајем никла су синтетисани сол-гел методом. Карактеризација узорака је извршена дифузном рефлексионом спектроскопијом и импедансном спектроскопијом користећи Мот-Шотки анализу. Редукција 4-нитропфенола је испитана на електроди од стакластог угљеника модификованој синтетисаним композитима. Модификација електроде од стакластог угљеника је довела до јаке привидне електрокатализе. Корелација између структурних, текстуралних и електрохемијских особина испитиваних композита је успостављена методом анализе главних компоненти.*

Кључне речи*: алумина, сол-гел процес, електрохемијска мерења, анализа главних компоненти.*